Elasto-Plastic Behaviour of Axially Loaded Filled Circular Steel Stub Columns

Walter O. Oyawa*, Kunitomo Sugiura** and Eiichi Watanabe***

* M.Sc.(Eng.), Graduate Student, Dept. of Civil Engrg., Kyoto University, Kyoto, 606-8501
** Ph.D., Assoc. Professor, Dept. of Civil Engrg. Systems, Kyoto University, Kyoto, 606-8501
*** Dr. of Eng., Ph.D., Professor, Dept. of Civil Engrg., Kyoto University, Kyoto, 606-8501

Extensive efforts in recent times have been focussed towards the evolvement and use of concrete-filled steel tubular structures in bridge piers and high-rise building columns. Such structures exploit the best attributes of both steel and concrete, resulting in higher stiffness, strength and ductility; particularly essential for earthquake resistance. Studies are presently being conducted on the structural response of filled steel composite members, by taking into account the effect of fill materials' properties. Findings of these studies relating to elasto-plastic response of filled steel stub columns under compressive load, indicate the potential of epoxies and carbonic grout as alternative fill materials to concrete or which could be combined with concrete for enhanced strength and ductility as well as reduced weight of filled steel members. From the viewpoint of promoting high ductility, strength of fill material should be limited e.g. to less than 10 N/mm^2; furthermore elastic modulus should be lower and, Poisson's ratio higher.

Keywords: *Filled steel columns, Stub column test, Elasto-plastic behaviour, Strength, Ductility*

1. Introduction

Looking ahead towards the uncertain challenges of the 21st century, the use of advanced materials in structural engineering or unprecedented combinations thereof is an area which is attracting intensified attention, as the construction industry grapples with the even more demanding requirement of safe and economical structures. One such application, gaining popularity in recent times, is the use of concrete-filled steel tubular structures in the construction and retrofitting of bridge piers and high-rise building columns[1,2,3,4]. It is well known that concrete-filled structures exploit the best attributes of both steel and concrete, thus allowing the engineer to maintain manageable member sizes while obtaining increased stiffness, energy absorption, strength and ductility; particularly essential for severe conditions of earthquake loading in seismic areas such as Japan[5,6,7].

In earthquake resistant design, it is aimed to provide members that will effectively absorb and dissipate energy through inelastic deformations of low amplitude or hysteretic damping, (without severe damage to the structure), thereby reducing the ductility demand on the structure. When a member is of high ductility, substantial reduction in the design seismic load is admissible. Further still, concrete-filled tubular members provide a better fireproofing and soundproofing property than steel structures, and are even easier, safer, and faster to construct. Thus, the superiority of concrete-filled steel composite members when used in earthquake resistant structures can not be over-emphasized. Of interest maybe the possibility of evolving appropriate advanced materials for use as alternative fill materials.

In light of the severe structural damage caused by the 1995 Hyogoken-Nanbu Earthquake in Japan, studies are presently being conducted on the performance of various types of filled steel composite members e.g. retrofitting method involving filling of steel tubular piers to enhance ductility only, in an attempt to supplement efforts geared towards evolving earthquake resistant structures. Findings of these studies, namely the effects of various characteristics of non-conventional types of fill materials on structural response of filled steel stub columns under compressive load, are presented herein in conjunction with the local instability of steel tube.

2. Experimentation

2.1 Scope of investigations

Several types of circular steel composite columns filled with various types of fill materials were gradually subjected to axial compressive load until failure, while recording load, strain and displacement measurements at suitable increments, by using test setup shown in Fig. 1.

The circular test specimens (see Fig. 2) were classified into four categories depending on specimen sizes (expressed as radius to thickness ratios i.e. D/2t). Each series consisted of circular steel composite specimens filled with Carbonic grout cured for 6 days (C1), Carbonic grout cured for 25 days (C2), Rubber (R), Rubber Bits (RB) glued or bound together by urethane resin, a stiff Epoxy type (E1) and a flexible Epoxy type (E2). In addition, for each composite member corresponding separate components were prepared and similarly tested. To facilitate identification, test specimens were designated according to material type and the value of radius to thickness ratio expressed as D/2t ratio. For example, S/C2-40 implies circular steel (S) filled with carbonic grout cured for 25 days (C2), and of D/2t ratio equal to 40. To provide a flat contact surface during testing, the top and bottom surfaces of the specimens were machine ground. However, end friction during testing was not eliminated. Table 1 illustrates the details of the specimens.

Before commencing tests, longitudinal and horizontal strain gages were pasted around the middle circumference of each specimen. Each specimen was in turn placed centrally on the bottom loading platen of TKS Universal Testing Machine and four linear variable displacement transducers (LVDTs) for vertical deformation between the loading heads, fixed equidistant around the specimen. All the data measuring equipment were connected to a data logger, which was in turn connected to a computer. Testing then commenced and proceeded by gradual application of axial compressive load and at suitable load increments, readings of load, displacement and strain were taken and recorded by computer.

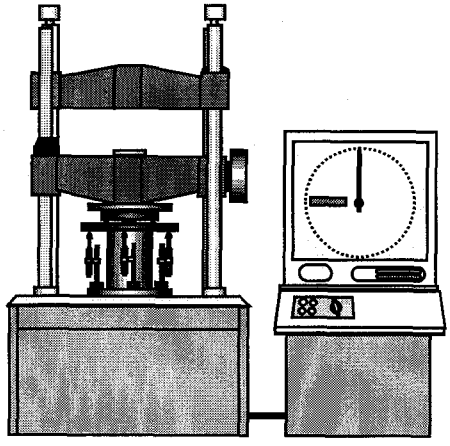

Figure 1. Stub column test setup

2.2 Material properties

Material properties for the different thickness of steel were determined from tensile tests on strips cut from steel sheets used to form the tubes. Results, shown in Table 2 and Fig. 3, were also used to normalize and evaluate test results obtained for the composite and steel circular specimens.

The main material properties for the fill materials, determined from cylinder compression tests, are presented in Table 3 and Fig. 4. Young's modulus and Poisson's ratio have been determined using strains measured by the more localized hence more accurate strain gages, and not from the average shortening strains measured by LVDTs. The unit weight of fill materials is the weight of the specimens per unit volume, while the bulk modulus, regarded as a measure of incompressibility, has been determined from the expression $K = E/3(1-2\nu)$, where E is the Young's modulus and ν the Poisson's ratio. It is noted that the two types of carbonic grout have properties closer to concrete, since they are actually derivatives of concrete. Epoxy and rubber types, on the other hand, have much higher Poisson's ratio and much lower Young's modulus than steel. Epoxy E2 has the highest bulk modulus despite its very low Young's modulus, indicating incompressibility with high capability of outward flow among all the fill materials considered herein. During the compressive tests, ultimate strengths of epoxy E2 and rubber specimens could not be attained within the usual range of strain measurements, and hence nominal ultimate strengths were specified at the very high axial shortening strains of 8% to 10%. Upon release of compressive load, epoxy E2 and rubber specimens recovered most of their deformations. Failure of carbonic grout specimens was by formation of longitudinal shear cracks as in the case of concrete. In contrast, epoxy E1 failed by formation of a bulging head, which then burst open forming a crack line.

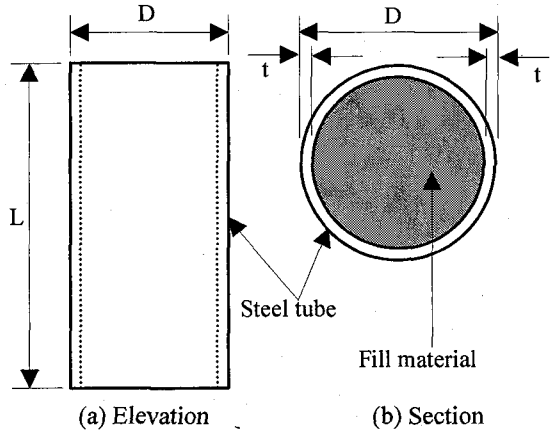

(a) Elevation (b) Section

Figure 2. Filled steel stub column specimen

Table 1. Stub column specimen details (nominal)

Specimens identification	L (mm)	D (mm)	t (mm)	D/2t	Area of steel A_s (mm^2)	Area of fill A_{fill} (mm^2)	A_{fill}/A_s
(S/C1,S/C2,S/R,S/E1,S/E2,S/RB)-20	208	104	2.6	20	828.2	7667	9.3
(S/C1,S/C2,S/R,S/E1,S/E2,S/RB)-30	192	96	1.6	30	474.5	6764	14.3
(S/C1,S/C2,S/R,S/E1,S/E2,S/RB)-40	192	96	1.2	40	357.4	6881	19.3
(S/C1,S/C2,S/R,S/E1,S/E2,S/RB)-50	200	100	1.0	50	311.0	7543	24.3

Nomenclature: Specimen identification e.g. S/C2-40 implies composite stub column specimen of steel (S) filled with carbonic grout type 2 (C2), and of D/2t ratio equal to 40.

Table 2. Properties of steel

Thickness (mm)	Young's modulus (KN/mm^2)	Poisson's ratio	Yield stress (N/mm^2)	Ultimate strength (N/mm^2)	Elongation at break (%)	Bulk modulus (KN/mm^2)
2.6	215	0.287	231	352	46.6	168
1.6	216	0.337	225	325	46.9	221
1.2	198	0.357	189	318	47.8	231
1.0	211	0.337	230	340	42.9	216

Table 3. Properties of the fill materials

Fill material description	Fill material designation	Unit weight (Kg/m^3)	Young's modulus (KN/mm^2)	Poisson's ratio	Ultimate strength (N/mm^2)	Bulk modulus (KN/mm^2)
Carbonic grout-EA	C1	1897	11.9 (0.057)*	0.239 (0.72)*	14.5 (0.07)*	7.60 (0.036)*
Carbonic grout-OA	C2	1843	13.1 (0.062)	0.222 (0.67)	21.1 (0.1)	7.85 (0.038)
Rubber	R	1018	0.0014 (0.000007)	0.455 (1.38)	>0.1**(0.0005)	0.005(0.00002)
Epoxy-HS	E1	1211	1.6 (0.008)	0.424 (1.28)	41.2 (0.19)	3.51 (0.017)
Epoxy-LS	E2	1134	1.1 (0.005)	0.484 (1.47)	>8.8** (0.04)	11.46 (0.055)
Rubber Bits	RB	729	0.0379 (0.0002)	0.456 (1.38)	>0.25**(0.001)	0.144 (0.0007)

* The values in brackets are corresponding ratios to Young's modulus, Poisson's ratio, yield stress and bulk modulus of steel
**The strengths of fill materials R, E2 and RB have been stated at 8 %, 10 %, and 10 % axial shortening strains respectively

Abbreviations

EA-Early age (6 days) OA-Ordinary age (25 days)

HS-High strength LS-Low strength

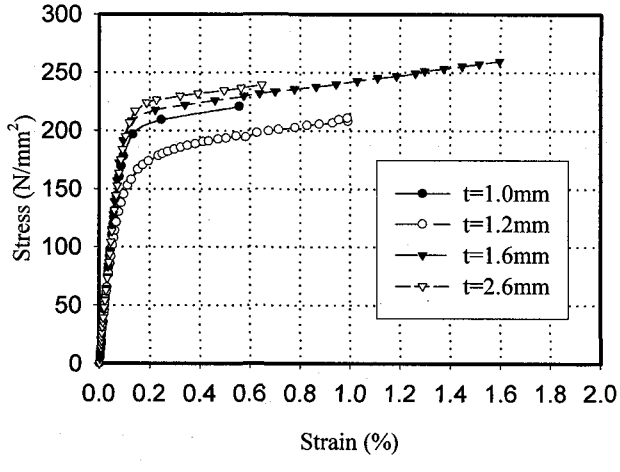

Figure 3. Tensile stress-strain relations of steel strips of different thickness (t)

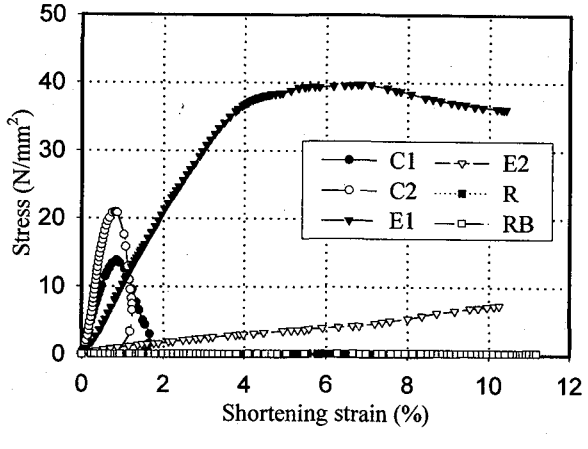

Figure 4. Compressive stress-strain relations for the fill materials (shortening measured by LVDTs)

3. Results and Discussion

3.1 Load-strain characteristics

Figures 5 and 6 relate non-dimensional force to non-dimensional shortening of the filled composite and empty steel stub column specimens. The axial shortening has been normalized by shortening at yield of steel (u_y) while axial force has been normalized by steel axial yield force (P_y) as in Fig. 5, and sum of strength of separate components (Psum) as in Fig. 6. Whereas Fig. 5 mainly presents force-deformation behaviour of the different specimens, Fig. 6 provides an insight into the confinement effect on the fill materials by the steel tube, hence the extent of composite action. Increased strength of composite member due to confinement of the fill material is most evident in carbonic grout filled steel specimens, where there is a smooth transition from elastic region to plastic zone. In contrast, the confining action is most diminished in the case of epoxy E1 as indicated by abrupt change of gradient of its curve in Fig. 6, attributable to its comparatively high compressibility as represented by its relatively low value of bulk modulus.

Considering only Fig. 5, several distinct patterns of force-displacement relation are observed depending on the type of fill material. Epoxy E1-filled steel stub column (S/E1) has 3 response regions; a linear portion up to just above the yield load of steel section (P_y), another linear portion of reduced stiffness and finally a flat portion. The trend suggests that as loading process begins on specimen S/E1, the steel supports most of the applied load until its yield point owing to its higher Young's modulus. Soon the tangent modulus of the intensely stressed steel tube reduces significantly, limiting its load resistance capacity. After the initiation of yielding of steel tube, there is redistribution of load with a higher percentage of the applied load being transferred to epoxy E1 with low Young's modulus which, due to its low bulk modulus, is also less sensitive to confinement by steel tube, hence the observed abrupt reduction in slope or stiffness of the composite member after yielding of steel tube. The moderately confined epoxy E1 initially resists the load linearly and then converts to the curved path of plastic deformation with the steel tube undergoing extensive buckling deformations with a little decrease in the global stiffness and confinement action. Eventually, the maximum load is attained and the composite stub column continues to deform at a near constant load, with the confined epoxy compensating for the degradation in steel after buckling. Finally, degradation of S/E1 occurs due to failure of epoxy E1 as explained in section 3.2.

On the other hand, epoxy E2-filled steel stub column (S/E2) has a response which uniquely stands-out in the elastic region; there is marked decrease in the stiffness of the filled composite due to lateral pressure exerted by E2. This rare phenomenon is thought to be directly related to the high bulk modulus of epoxy E2 compounded with its high Poisson's ratio; properties which suggest high incompressibility as well as high capability of outward bound flow of epoxy E2, reminiscent of viscous flow of fluids. However, as loading proceeds the properties of E2 transform resulting in improvement in its load resistance capacity. Composite load sharing action with the steel tube is initiated, and when the steel buckles, applied load is fully transferred to epoxy E2. The confined epoxy supports the increasing load and ultimate load is never attained.

Use of Rubber as a fill material seems to have minor effect and the Rubber-filled steel stub columns i.e. S/R and S/RB specimens, have a response much closer to that of hollow steel, attributable to the very low bulk and Young's moduli of rubber. The minor effect is that the presence of rubber slightly reduces the stiffness of steel in a similar fashion to epoxy E2, due to its high Poisson's ratio.

Carbonic grout-filled steel stub columns (S/C1 and S/C2 specimens) have an overall response different from that of the epoxies or rubbers, but more representative of concrete-filled steel members. In the early stages of loading, the carbonic grout is not initially restrained laterally by the steel tube because it has a lower Poisson's ratio than steel. Hence the steel tube and carbonic grout initially resist the applied load independently, each according to its Young's modulus and cross-sectional area. However, as loading progresses carbonic grout expands catching up with the steel tube. Previous studies on concrete-filled steel members[8,9,10] have shown that when concrete is loaded axially, initially the concrete decreases in volume but when the loading level approaches the strength of concrete, microcracking occurs accompanied by rapid volumetric expansion for small increase in stress. In other words, the effective Poisson's ratio of the concrete, or carbonic grout in the case of this study, rapidly increases to that of steel, even higher. Radial pressure is developed at the steel and carbonic grout interface, resulting in a confining action or triaxial stress condition in carbonic grout, with consequent increase in strength and possibly effective modulus of elasticity of the confined carbonic grout[11,12]. Since carbonic grout is comparatively incompressible as indicated by its high bulk modulus, composite action is initiated as the confined carbonic grout and the steel share the applied load. It may be observed that the linear portion of the graph extends well beyond the steel yield load due to this composite action. As loading continues, it is postulated that the steel tube yields with most of the load being transferred

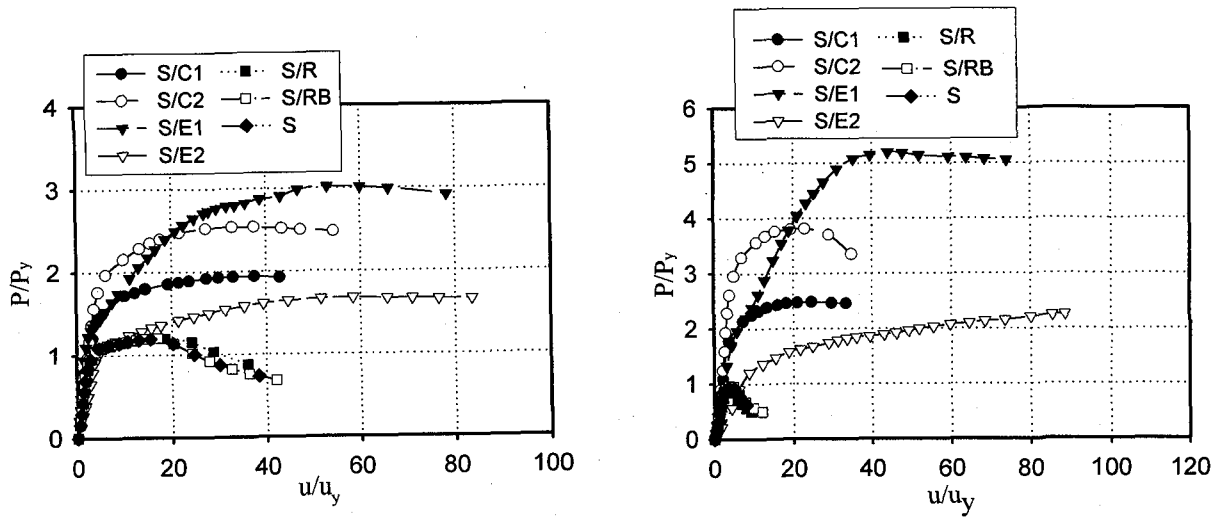

(a) D/2t=20 (b) D/2t=50

Figure 5.Non-dimensionalized load versus axial displacement, normalized by steel yield load

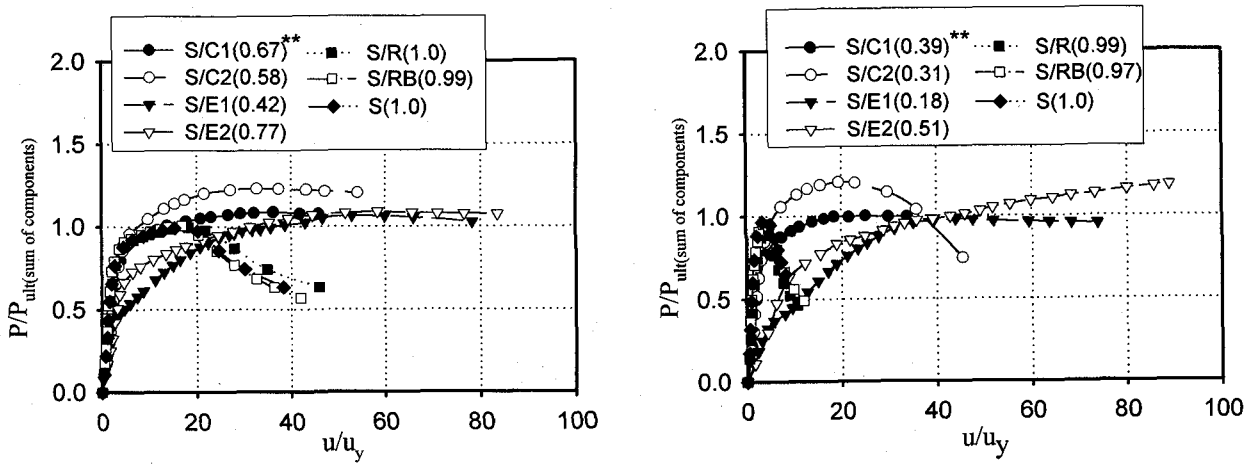

(a) D/2t=20 (b) D/2t=50

Figure 6. Non-dimensionalized load versus axial displacement, normalized by sum of strength of components
(**Values in brackets represent the ratio $P_{ult(Steel)}/P_{ult(sum\ of\ components)}$)

to the carbonic grout. When carbonic grout fractures, buckling deformations in the steel tube are accelerated as indicated by the curved and near flat portions of the graph. The extent of deformations after the ultimate load is attained depends on D/2t ratio as seen in Figs. 5(a) and 5(b).

3.2 Modes of failure

Photos 1 and 2 illustrate the different modes of failure of the filled steel specimens, which have been split into two for better view. Extensive damage is evident in the epoxy-filled specimens shown in Photo 1 where, in addition to the usual end buckling waves, there are intermediate waves caused by extensive radial expansion of the fill material. For the filled-in epoxy E1 failure is depicted in the form of longitudinal cracks, which may have been caused by tensile bursting forces; a mode of failure which was also observed during uniaxial material property test. Filled-in epoxy E2 remains stable and uncracked, consistent with its basic material property of high deformation capability with no definite ultimate load within the usual strain measurements. It is also noted that there is negligible adhesion between the steel tube surface and the filled-in epoxy, since the two pieces can be separated quite easily.

Carbonic grout-filled stub columns have only the end buckling deformations as seen in Photo 2. The buckled portions of the steel tube present sufficient space for parts of the carbonic grout to expand leading to fracture. The fracture is propagated diagonally in a shear kind of failure whereby shear cracks extend diagonally from the fracture points in an apparent attempt to connect the opposite fracture zone in the case of D/2t=50. The bonding of carbonic grout and the steel tube surface is firm, unlike the case of epoxy-filled steel stub columns.

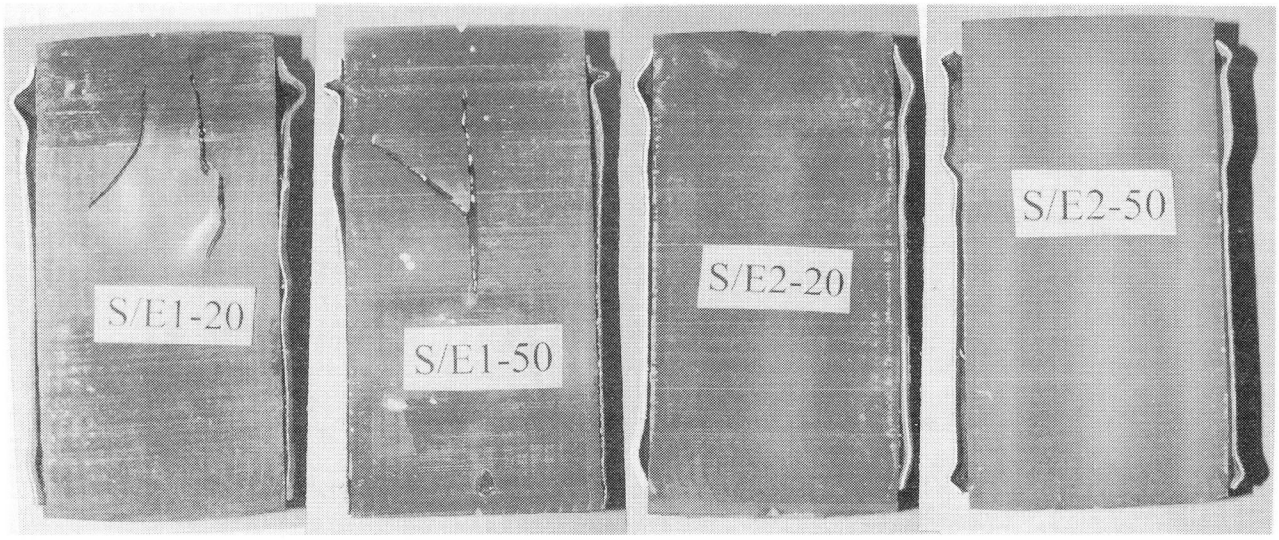

Photo 1. Epoxy filled-steel specimens split after test

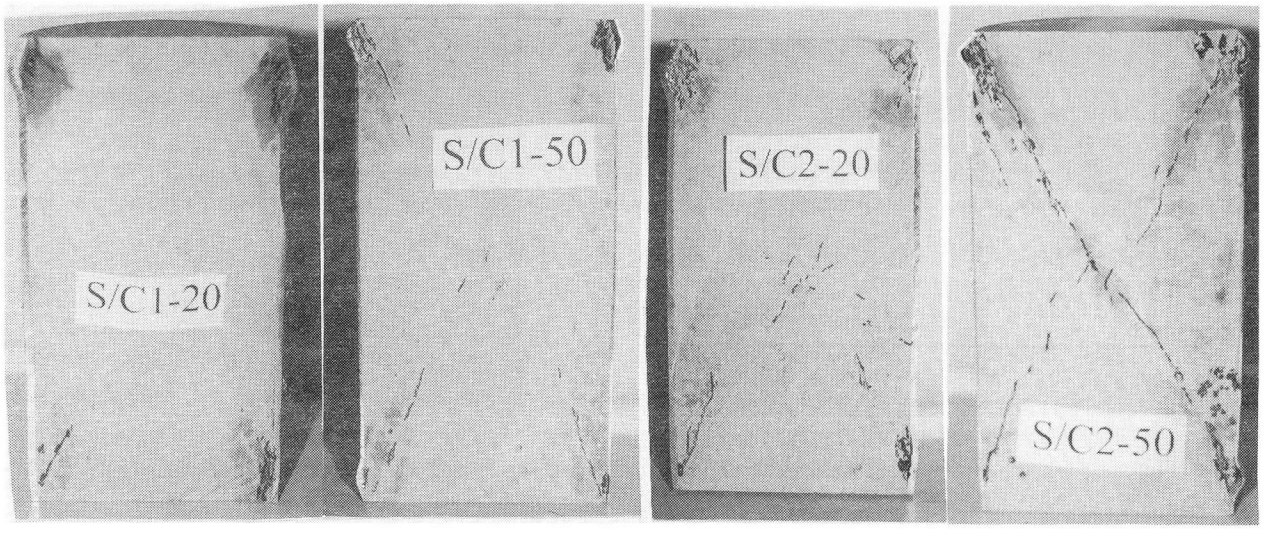

Photo 2. Carbonic grout filled-steel specimens split after test

3.3 Elasto-plastic biaxial stress path of steel tube

In determining the elasto-plastic biaxial stress relations from the measured vertical and horizontal strains in the steel tube, several formulae were employed[13]. For the elastic range, the axial (designated direction z) and hoop (designated direction h) stresses σ_{sz} and σ_{sh} respectively, induced in the steel tube have been calculated as below:

$$\sigma_{sz} = \frac{E_s}{1-\nu_s^2}\left(\varepsilon_{sz} + \nu_s \varepsilon_{sh}\right) \tag{1a}$$

$$\sigma_{sh} = \frac{E_s}{1-\nu_s^2}\left(\varepsilon_{sh} + \nu_s \varepsilon_{sz}\right) \tag{1b}$$

where ε_{sz} and ε_{sh} are the measured axial and hoop strains respectively, and E_s and ν_s are the modulus of elasticity and Poisson's ratio of steel respectively.

The yielding surface adopted is that due von Mises yield criterion in the biaxial principal stress state:

$$\left(\frac{\sigma_{sz}}{\sigma_{sy}}\right)^2 - \left(\frac{\sigma_{sz}}{\sigma_{sy}}\right)\bullet\left(\frac{\sigma_{sh}}{\sigma_{sy}}\right) + \left(\frac{\sigma_{sh}}{\sigma_{sy}}\right)^2 = 1.0 \tag{2}$$

in which σ_{sy} is the yield stress of steel.

For the elasto-plastic region, plastic flow equations according to Prandtl-Reuss have been employed, which may be represented in the incremental form simply as:

$$\sigma_{sz} = \sigma_{sz} + \Delta\sigma_{sz} \tag{3a}$$

$$\sigma_{sh} = \sigma_{sh} + \Delta\sigma_{sh} \tag{3b}$$

The incremental stress are obtained from incremental strains in the matrix formulation illustrated below:

$$\begin{Bmatrix} \Delta\sigma_{sz} \\ \Delta\sigma_{sh} \end{Bmatrix} = [D_{ep}] \begin{Bmatrix} \Delta\varepsilon_{sz} \\ \Delta\varepsilon_{sh} \end{Bmatrix} \quad (4)$$

where $[D_{ep}]$ is the elasto-platic stress-strain stiffness matrix given as follows:

$$[D_{ep}] = \frac{E_s}{1-\nu_s^2} \begin{bmatrix} 1 & \nu_s \\ \nu_s & 1 \end{bmatrix} - \frac{1}{S} \begin{bmatrix} S_1^2 & S_1 S_2 \\ S_1 S_2 & S_2^2 \end{bmatrix} \quad (5)$$

in which S, S_1 and S_2 are defined as follows, assuming perfect plasticity in steel;

$$S = S_1 \sigma_{sh}' + S_2 \sigma_{sz}' \quad (6a)$$

and

$$S_1 = \frac{E_s}{1-\nu_s^2} (\sigma_{sh}' + \nu_s \sigma_{sz}') \quad (6b)$$

$$S_2 = \frac{E_s}{1-\nu_s^2} (\nu_s \sigma_{sh}' + \sigma_{sz}') \quad (6c)$$

where σ_{sh}' and σ_{sz}' are stress deviators in the horizontal and vertical directions.

The stress paths of empty and composite filled steel tubes are presented in Figures 7 to 9. Several distinct points A,B,C and D have been marked for easy identification on the graphs for fill material stress path in the next section.

For epoxy-filled steel stub columns it is observed that the response of epoxy E1-filled steel is quite different from that of epoxy E2-filled steel. In Fig. 8(a), E1-filled steel has a vertical path of elastic response showing that there is negligible hoop stress in the steel i.e. most of the applied axial load is resisted by the steel due to the much lower modulus of elasticity of E1. The steel then yields at point A, redistributing the applied load to epoxy E1 as indicated by the drop along the von Mises yield surface. It may be noted that increased load on the fill material E1 leads to its increased lateral deformations, hence the observed increase in steel hoop stress while vertical load decreases. Further loading induces a sudden surge in horizontal stress, perhaps caused by sudden bursting out failure of epoxy E1 when restrained by stronger steel section. It may be stated that during material property tests, epoxy E1 failed by bursting tensile cracks.

In contrast, the path for epoxy E2-filled steel as seen in Fig. 8(a), shows a very high initial hoop stress in the steel tube, which as previously mentioned could be explained by the very high bulk modulus compounded with high Poisson's ratio of epoxy E2. The very high bulk modulus of E2 together with its very high Poisson's ratio suggest that E2 has characteristics tending towards liquids, i.e. high incompressibility but with high capability of flow. Thus, as soon as loading commences, the fill material E2 exerts lateral pressure on the steel tube, causing it to extend laterally outwards while bulging. However, as loading continues properties of E2 change enabling composite interaction or sharing of load between the steel tube and E2. The steel partially yields at point A, but continues to support load as its path closely follows the von Mises yielding surface in an ascending direction. At some point B the steel tube begins to buckle when the vertical stress in it equals the steel axial yield stress, and the path reverses and takes a descending direction. At this point, the entire applied load in the tube begins to be transferred to the fill material, as buckling of steel proceeds significantly. The two kinds of Carbonic grout-filled steel stub columns show a similar pattern as that of epoxy E1, with some hoop stress in the steel within the elastic range, confirming early interaction of carbonic grout and steel surface. The steel yields transferring most of its load to the carbonic grout and the path taken approximates the yield surface in a descending direction similar to epoxy E1-filled steel stub columns.

A rather distinct feature of the curves is the effect of D/2t ratio. It is generally observed that stub columns with a D/2t=50 have plastic stress paths which, although are parallel to the von Mises surface, are within the presumed elastic range of von Mises surface, and not wholly along the yield surface. This may be attributed to premature failure by buckling along the longitudinal length of these thin sections (with a thickness of 1.0 mm). Fig. 7 of empty steel tube most clearly illustrates the effect of D/2t ratio. The plastic flow path for D/2t=20 is ascending along the yield surface due to strain hardening before descending again because local instability causes the extension of cross-section. In the case of D/2t=50, the plastic path descends just below the von Mises yield surface because of local buckling.

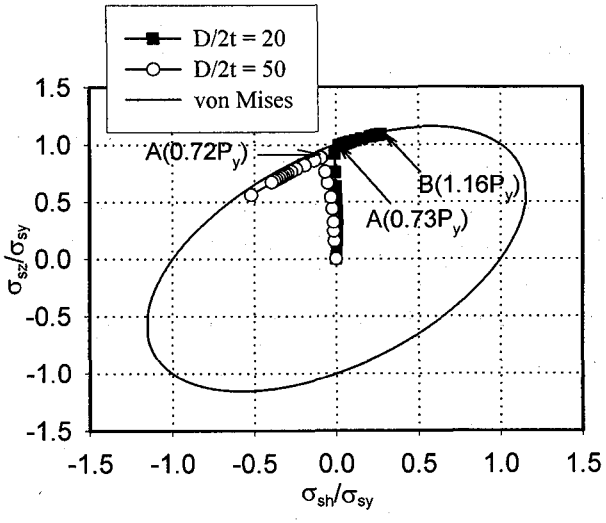

Figure 7. Stress path of empty steel stub columns

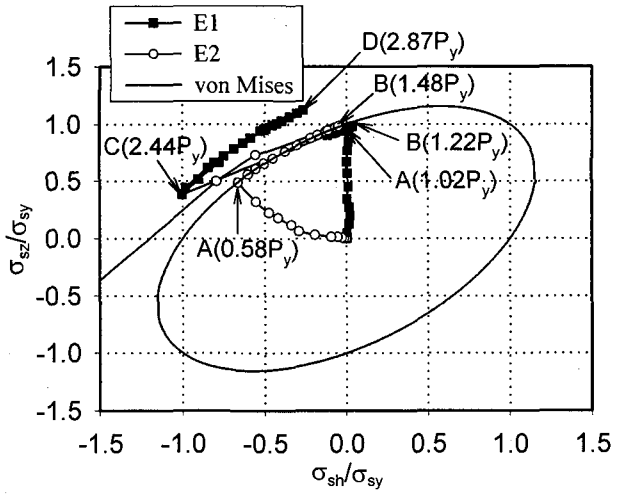

(a) D/2t=20

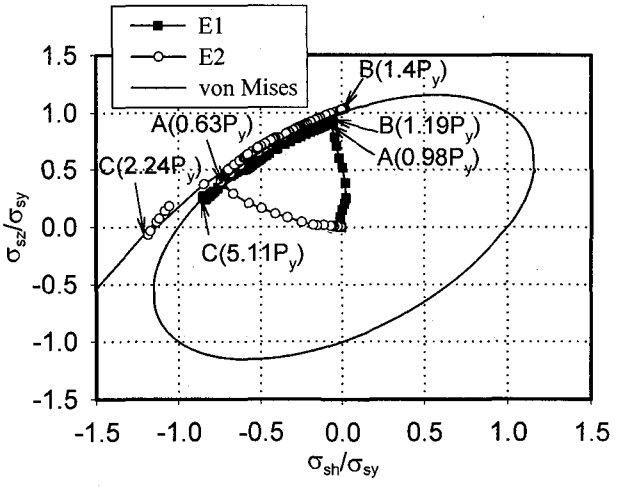

(b) D/2t=50

Figure 8. Stress path of steel, in epoxy-filled steel stub columns

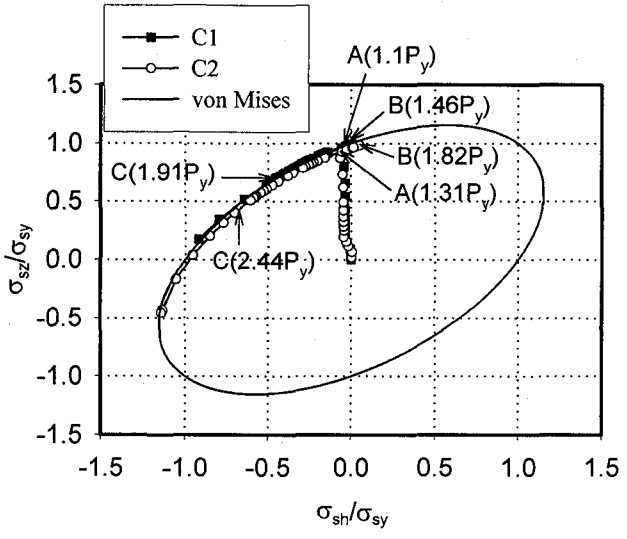

(a) D/2t=20

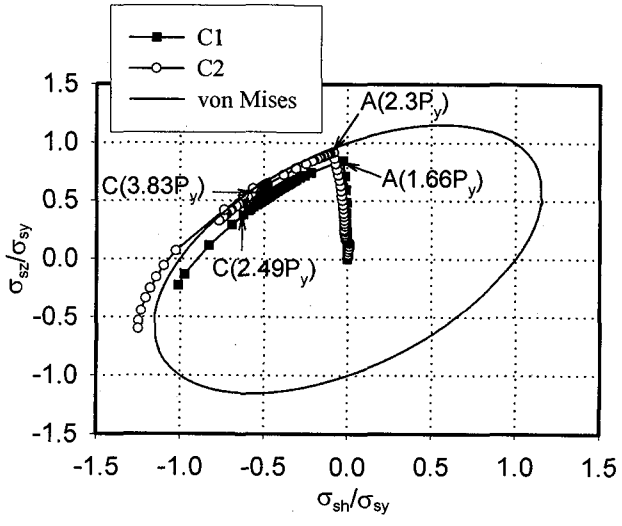

(b) D/2t=50

Figure 9. Stress path of steel, in carbonic grout-filled steel stub columns

3.4 Stress path of fill material subjected to triaxial stress

The influencing stress conditions on fill material, which is confined by the steel tube, are taken to be the hydrostatic stress condition represented as the first stress invariant (I_1), and the shearing stress, related to the square root of the second invariant of stress deviator ($\sqrt{J_2}$). Hence, a relationship involving the two parameters illustrates the stress path in the fill material. Quantities calculated from the mathematical formulae presented below were plotted in the Cartesian axes, to depict the stress path in the confined fill materials;

$$\sqrt{J_2} = \frac{|\sigma_{fh} - \sigma_{fz}|}{\sqrt{3}} \tag{7}$$

$$I_1 = \sigma_{fz} + 2\sigma_{fh} \tag{8}$$

The lateral and axial stresses on the fill material are derived from the strains measured on the steel surface, respectively as below;

$$\sigma_{fh} = -\frac{2t}{D_i}\sigma_{sh} \tag{9}$$

$$\sigma_{fz} = \frac{P - \sigma_{sz} A_s}{A_c} \tag{10}$$

where D_i : internal diameter of the steel tube

t : thickness of the steel tube

P: applied axial compressive load

A_s and A_c : sectional areas of steel and fill material

The stress paths for epoxy and carbonic grout inside the steel tube are presented in Figs. 10 and 11, and largely corroborate previous discussions for the stress paths of steel. The points A, B, C and D correspond to locations on the steel tube stress path given in Figs. 8 and 9, while the

horizontal dashed line marks the apparent uniaxial strength of the unconfined fill material. Stresses above this line show the additional strength acquired by the fill materials as a result of the confining action of the steel tube.

The path of epoxy E1 reverses soon after the graph crosses the uniaxial compressive strength line, indicating that the confined strength of epoxy E1 is not very different from its unconfined strength (Fig. 10a). This observation is in line with previous discussions, whereby it was stated that low bulk modulus hence high compressibility of epoxy E1 counteracts the confining action of the surrounding steel until after the steel has buckled extensively. There is less confining action on the epoxy by the buckled steel. Points A and B mark the yielding point and maximum load in the steel tube, respectively. The points occur quite low on the graph confirming that by the time the maximum load of the filled steel column is attained, the steel tube is extensively damaged. Epoxy E2 with high bulk modulus and high Poisson's ratio behaves initially more like confined fluid and hence there is minimal shear stress initially as depicted by the horizontal flow in the stress path (Fig. 10b). As loading proceeds the properties of E2 change resulting in increased load resistance capacity and hence when the steel yields at point A, the graph is seen to shift towards the uniaxial compression line.

The stress path of carbonic grout shows a marked increase in strength of the confined fill material above the uniaxial strength due to effective confinement by the steel tube. Carbonic grout has high bulk modulus and low Poisson's ratio, hence composite interaction with the steel is initiated more significantly only after the steel has yielded as marked by point A, whereby load is shared thus relieving intensity of load on the steel while the steel confines it. A change of slope into plasticity region occurs near or above the uniaxial strength, giving a relation approximating that of Drucker-Prager type[13] concrete plasticity model, which assumes a linear relation between $\sqrt{J_2}$ and I_1.

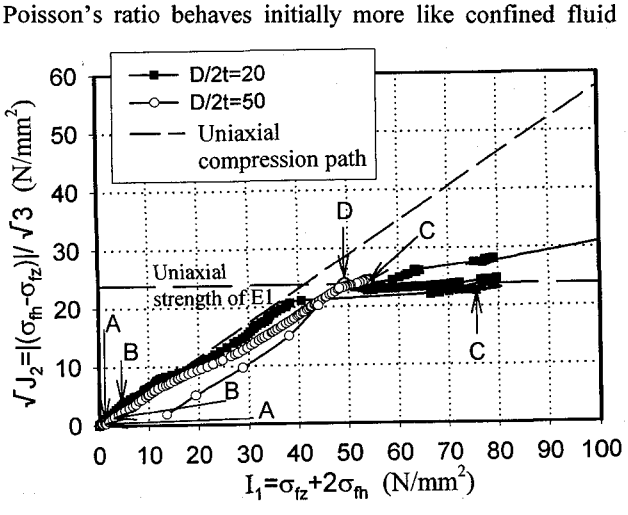

(a) Epoxy E1

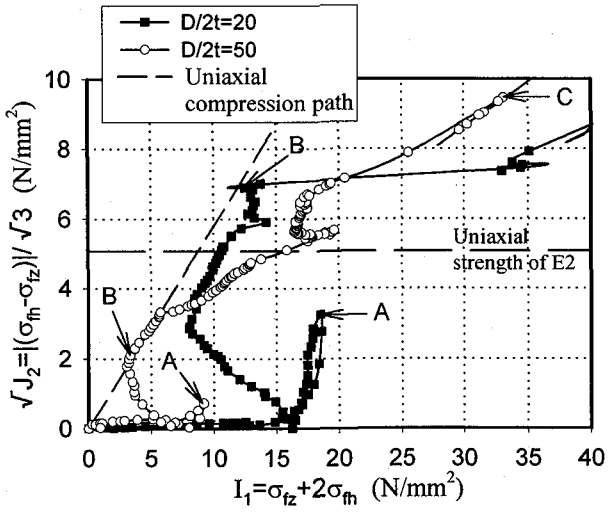

(b) Epoxy E2

Figure 10. Stress path of epoxy, which is confined by steel tube

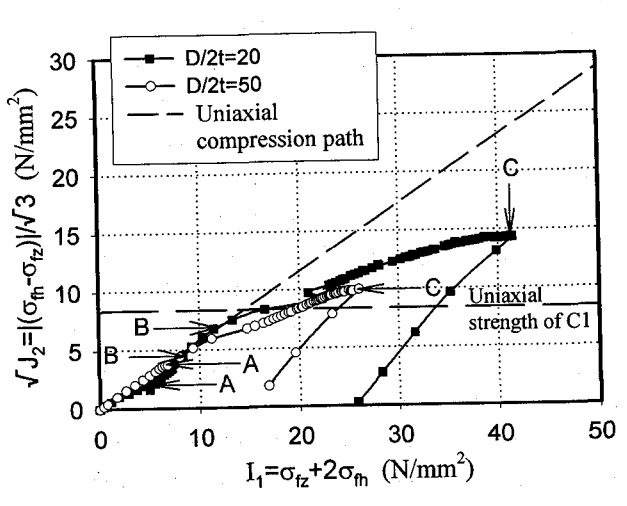

(a) Carbonic grout C1

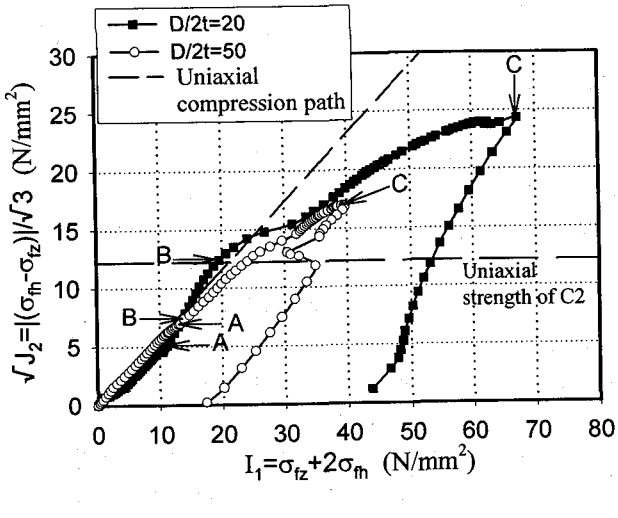

(b) Carbonic grout C2

Figure 11. Stress path of carbonic grout, which is confined by steel tube

3.5 Effects of fill material on Strength and ductility of composite column

Fig.12 shows that strength of composite stub columns in compression increases with increase in strength of the fill material as would be expected. The obtained results are further compared with those of concrete-filled steel stub columns from previous studies[14]. It is noted that there is an optimum strength of concrete after which there is negligible increase in normalized strength of the concrete-filled steel stub columns. Perhaps high strength concrete, owing to its brittleness and lower degree of volumetric expansion, is less sensitive to confinement effect of the steel tube. Fig. 13 indicates that the strength benefit accrued from the composite action of steel and fill material (expressed as the ratio ultimate load of composite column to the sum of the separate ultimate loads of the corresponding components) depends not only on strength of fill material but on a combination of other factors, possibly Poisson's ratio, bulk modulus of the fill material and D/2t ratio of the steel. Hence, the response of epoxy-filled steel columns is quite different from the response of carbonic grout-filled steel columns due to their widely different properties. The comparatively lower confining effect for Epoxy E1 filled steel columns despite the high strength of E1 is due to its much lower bulk modulus, as previously discussed. Lower bulk modulus implies high compressibility, hence the confining steel tube buckles before strain large enough to develop the maximum strength of E1 is attained. The effect of Poisson's ratio is illustrated in Fig.14, and also shows mixed order of response.

For either of the graphs, when the results of S/E1 are considered there are lines inconsistently crossing each other indicating that steel tubes with D/2t=40 and D/2t=30 give the highest strength benefit for S/E1 stub columns, respectively. It is imagined that this could be due to the effect of different strengths of the steel tube on the mode of failure of epoxy E1. Tests for steel material properties given in Table 2 show that the tube with D/2t=40 had comparatively lower yield and ultimate strengths, followed by the tube with D/2t=30. Since, the uniaxial mode of failure of E1 is mainly by bulging of the top portion followed by bursting cracks, these lower strength tubes may be better placed to permit epoxy E1 to expand or bulge, attaining higher strength. In contrast, high strength tubes could limit the bulging of E1, perhaps restricting it to the more rapid shear kind of failure.

Effects of fill material properties on ductility are illustrated in Figs. 15 to17. Ductility in these evaluations is defined by normalized displacement at the peak of the load-displacement curve of the stub columns. Strength of the fill material does not have a unique correlation with ductility as seen in Fig. 15, with the lower strength epoxy E2 producing a composite column of the highest ductility. If only ductility is to be improved, then the strength of fill material should be kept lower, such as less than 10 N/mm^2. It is evident that epoxy filled stub columns have the highest ductility owing to the high ductility of the epoxies which is best represented by their higher Poisson's ratio. It may be recalled that during material tests, epoxy E2 specimens never attained the stage of ultimate load and continued deforming at higher strains with increased load. Fig. 16 clearly illustrates that as Poisson's ratio increases, ductility likewise increases. Since the ultimate failure of the composite filled steel stub columns occurs only after the fill material has failed, it would be expected that the more ductile the fill material is, the more ductile the composite member containing the fill material is. Viewed in the reverse, the stiffer the fill material as represented by higher Young's modulus, the lower the ductility as can be seen in Fig. 17.

Generally, it is noted that fill material properties, namely strength, bulk modulus and Poisson's ratio significantly influence the response of filled steel stub columns. In this study a wide range for these parameters was made possible by the use of epoxies, rubbers and carbonic grout. It has been deduced that fill materials having extremes of these properties do not augur well for composite interaction with steel. An example is epoxy E1 whose high strength is counteracted by its low bulk modulus. Similarly, the very high bulk modulus of epoxy E2 is counteracted by its high Poisson's ratio.

Perhaps an ideal fill material for the construction of filled steel composite members should have properties somewhere in between epoxy and concrete, picking up the best attributes of epoxies and ordinary concrete e.g. high bulk modulus and moderate or optimum Poisson's ratio. However, in the case of retrofitting and rehabilitation where high ductility is particularly essential but not strength, epoxies present the best solution. A property of the epoxy materials, which could lead to significant reduction in seismic force, is their comparatively lower weight per unit volume. Epoxies E1 and E2 have weights per unit volume of 1211 Kg/m^3 and 1134 Kg/m^3 respectively, which are about half the weight per unit volume of ordinary concrete which is about 2300 Kg/m^3. Low weight materials not only reduce the design dead load, but are also easier to work on or handle during construction.

Nonetheless, before the structural contribution of the unique fill materials investigated in this study can be stated with certainty, further studies involving other forms of tests e.g. bending and cyclic tests are mandatory.

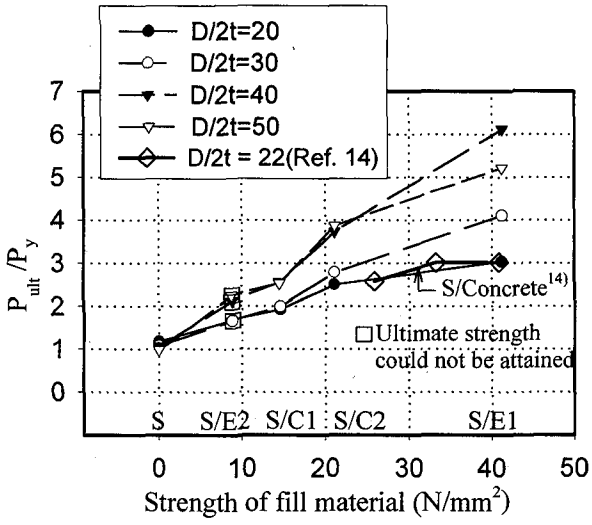

Figure 12. Effect of fill material strength on strength of composite column

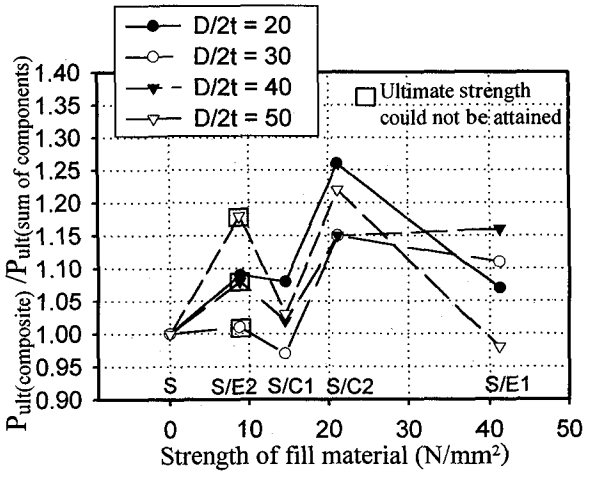

Figure 13. Effect of fill material strength on strength benefit of composite column

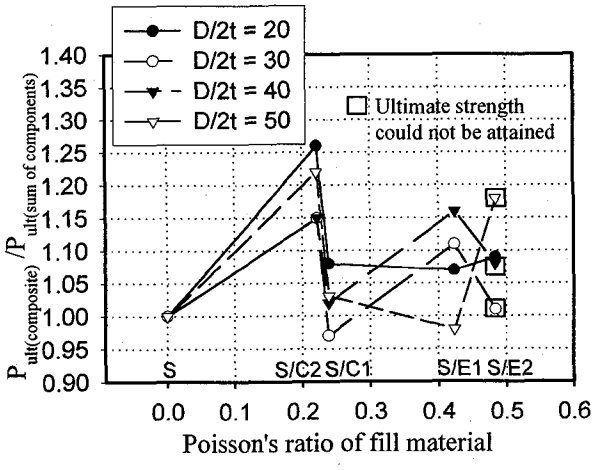

Figure 14. Effect of fill material Poisson's ratio on strength benefit of composite column

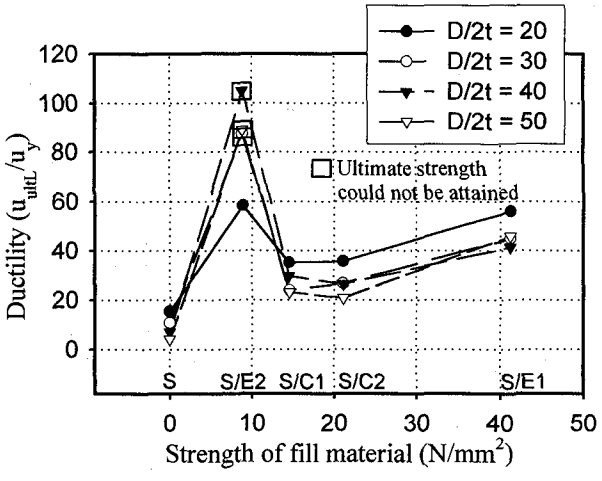

Figure 15. Effect of fill material strength on ductility of composite column

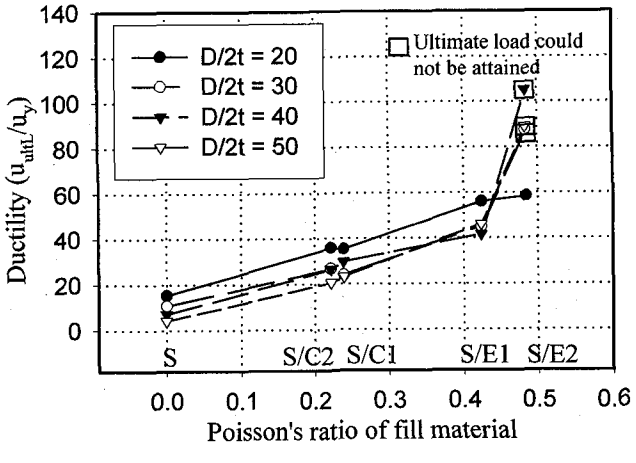

Figure 16. Effect of fill material Poisson's ratio on ductility of composite column

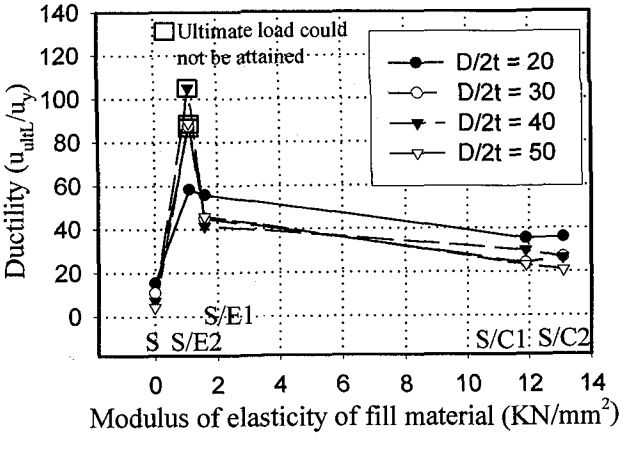

Figure 17. Effect of fill material modulus of elasticity on ductility of composite column

4. Conclusions

Potential alternative fill materials to concrete or which could be combined with concrete for enhanced strength and ductility as well as reduced weight of filled steel members have been identified. Particularly it is observed that Epoxy filled stub columns have considerably high ductility, when compared to ordinary concrete-filled steel members. Rubber has a negligible effect on filled steel stub columns.

Biaxial elasto-plastic stress path of the steel tube is assessed by assuming von Mises yield criterion. When the filled steel tube is of thinner thickness, premature failure of steel tube occurs below the yield strength caused by longitudinal shell buckling. The stress path of fill materials is also examined, and the amount of strength increase due to lateral confinement is quantified.

It is generally assessed that strength, bulk modulus and Poisson's ratio of the fill material significantly influence the response of filled steel stub columns. More specifically;

(a) high Poisson's ratio of the fill material results in high ductility of the composite member.

(b) high bulk modulus compounded with high Poisson's ratio as of super elastic fill material E2 rapidly degrades the effective stiffness of the composite member.

(c) regardless of Poisson's ratio, low bulk modulus implying high compressibility, counteracts and delays the confining effect of steel tube on fill material, thus minimizing the strength benefit accrued from composite action.

Perhaps an ideal fill material for composite construction could be somewhere in between epoxy and concrete, picking up the best attributes of epoxies and ordinary concrete e.g. high bulk modulus, moderate or optimum Poisson's ratio and low unit weight. However, for retrofitting and rehabilitation of structures where high ductility is particularly essential but not strength, which should be limited e.g. to less than 10 N/mm^2, epoxies present the best solution.

Acknowledgements

The authors wish to express their appreciation to the Kozai club for its financial encouragement. Appreciation is also extended to Nakaishoko, K.K. for their assistance in fabricating the test specimens.

References

1) Boyd, F.P., Cofer, W.F. and McLean, D.I., Seismic performance of steel-encased concrete columns under flexural loading, *ACI Struct. J.*, Vol. 92(3), pp. 355-364, 1995.

2) Bradford, M.A., Design strength of slender concrete-filled rectangular steel tubes, *ACI Struct. J.*, Vol. 93(2), pp. 229-235, 1996.

3) Azizinamini, A., Prakash, B. and Salmon, D.C., Force transfer mechanism for steel connection to tubes filled with concrete, 3rd Pacific Structural Steel Conference, JSSC, Tokyo, pp. 585-590, 1992.

4) Tang. J. Hino, S., Kuroda, I., and Ohta, T., Analytical study on elasto-plastic flexural behaviour of concrete-filled circular steel tubular columns, *Memoirs of the Faculty of Engineering*, Kyushu University, Vol. 57(1), pp. 37-52, 1997.

5) Ge, H. and Usami, T., Cyclic tests of concrete-filled steel box columns, *J. Str. Engrg.*, ASCE, Vol. 120(10), pp. 1169-1177, 1996.

6) Usami, T. and Ge, H., Ductility of concrete-filled steel box columns under cyclic loading, *J. Str. Engrg.*, ASCE, Vol. 120(7), pp. 2021-2040, 1994.

7) Elnashai, A.S., Broderick, B.M. and Dowling, P.J., Earthquake-resistant composite steel/concrete structures, *The Structural Engineer*, Vol. 73(8), pp. 121-132, 1995.

8) Imran, I and Pantazopoulou, S.J., Experimental study of plain concrete under triaxial stress, *ACI Materials. J.*, Vol. 93(6), pp. 589-601, 1996.

9) Furlong, R.W., Strength of steel-encased concrete beam columns, *J. Str. Engrg.*, ASCE, Vol. 93(ST5), pp. 113-124, 1967.

10) Knowles, R.B. and Park, R., Axial load design for concrete filled steel tubes, *J. Str. Engrg.*, ASCE, Vol. 96(ST10), pp. 2125-2153, 1970.

11) Kitada, T., Ductility and ultimate strength of concrete-filled steel members, Stability and ductility of steel structures under cyclic loading, edited by Fukumoto, Y. and Lee, G.C., *CRC Press*, London, pp. 139-148, 1992.

12) Usami, T., Mizutani, S., Aoki, T., and Itoh, Y., Steel and concrete-filled steel compression members under cyclic loading, Stability and ductility of steel structures under cyclic loading, edited by Fukumoto, Y. and Lee, G.C., *CRC Press*, London, pp. 123-138. 1992.

13) Chen, W.F. and Han, D.J., Plasticity for structural Engineers, Springer-Verlag, New York, pp. 72-84, 1988.

14) Gardner, N.J. and Jacobson, E.R., Structural behaviour of concrete filled steel tubes, *ACI J.*, Vol. 64(7), pp. 404-413, 1967.

(Received September 26, 1997)